Virology 418 (2011) 133–143

Contents lists available at ScienceDirect

Virology

journal homepage: www.elsevier.com/locate/yviro

Intrinsic disorder in the common N-terminus of human adenovirus 5 E1B-55K and its related E1BN proteins indicated by studies on E1B-93R

Timo Sieber [a,1], Roland Scholz [b,1], Michael Spoerner [c], Frank Schumann [c,2], Hans Robert Kalbitzer [c], Thomas Dobner [a,*]

[a] Heinrich Pette Institute, Leibniz Institute for Experimental Virology, 20251 Hamburg, Germany
[b] Department of Biology, Institute of Cell Biology, ETH Zurich, 8093 Zurich, Switzerland
[c] Institute for Biophysics and Physical Biochemistry, University of Regensburg, 93040 Regensburg, Germany

ARTICLE INFO

Article history:
Received 28 April 2011
Returned to author for revision 13 July 2011
Accepted 18 July 2011
Available online 17 August 2011

Keywords:
Adenovirus
E1B-55K
Intrinsically disordered proteins (IDPs)

ABSTRACT

The E1B transcription unit of human adenovirus encodes at least five different proteins generated by alternative splicing of a common E1B precursor mRNA. E1B-156R, -93R and -84R contain individual carboxy termini but share a common amino terminus. To acquire data on the structure of the amino terminus we performed biophysical analyses on E1B-93R. We show that E1B-93R is mostly unstructured and fulfills the criteria of an intrinsically disordered protein (IDP). The intrinsic disorder in the amino terminus of these proteins is evolutionary conserved in all seven human adenovirus species. As IDPs comprise a rapidly growing family of proteins which, despite their lack of a well defined structure, often fulfill essential regulatory functions, the observations described here might open up a new avenue for the understanding of the regulation and functions of E1B proteins, in particular the multifunctional E1B-55K oncoprotein.

Introduction

The gene products of the human adenovirus type 5 (HAdV5) early transcription unit 1B (E1B) fulfill essential functions for viral replication and adenovirus mediated cell transformation. The most prominent proteins, the 19 kDa E1B-19K (GenBank: AAQ19286.1) and the 55 kDa E1B-55K (GenBank: AAQ19287.1) are expressed from overlapping reading frames of the 2.28 kb E1B-mRNA (Fig. 1). Apart from this mRNA at least three additional mRNA forms are produced due to alternative splicing between a common splice donor (SD1) and one of three splice acceptor sites (SA1–3). The resulting mRNAs encode E1B-19K and E1B-55K-related proteins comprised of the 79 aa E1B-55K N-terminus and different C-termini. These factors are named E1B-156R (GenBank: JF430399), -93R (GenBank: JF430400) and -84R (GenBank: JF430401) due to their total number of amino acid residues (Anderson et al., 1984; Green et al., 1982; Lewis and Anderson, 1987; Lucher et al., 1984; Sieber and Dobner, 2007; Takayesu et al., 1994; Virtanen and Pettersson, 1985). While E1B-93R and E1B-84R contain unique C-termini, E1B-156R is completed by the last 77 residues of E1B-55K. As these proteins are structurally related by their N-terminus we termed them "E1BN proteins". This common N-terminus encompasses a characteristic region that is recognized as a conserved domain by NCBI (pfam04623 Adeno_E1B_ 55K_N).

E1B-19K and E1B-55K fulfill important tasks in viral infection and can individually cooperate with the adenoviral E1A (early transcription unit 1A) proteins to convert primary rodent cells to a fully transformed tumorigenic phenotype (Cuconati and White, 2002; Shenk, 2001; White, 2001). E1B-55K performs its multiple functions via interactions with a large number of viral and cellular proteins (reviewed in (Blackford and Grand, 2009)). A central element for many of these functions seems to be E1B-55K's ability to act as substrate recognition unit for an E3-Ubiquitin-Ligase composed of viral – E1B-55K and E4orf6 (gene product of HAdV5 early transcription unit 4 open reading frame 6) – and cellular factors (Blanchette et al., 2004; Harada et al., 2002; Querido et al., 2001). This complex is able to recruit and promote degradation of several cellular proteins including p53, Mre11 (meiotic recombination 11) DNA-Ligase IV and Bloom's helicase (Baker et al., 2007; Mohammadi et al., 2004; Orazio et al., 2011; Stracker et al., 2002). Further, we could recently show that E1B-55K can promote degradation of cellular Daxx (death domain-associated protein) independent of E4orf6 (Schreiner et al., 2010).

In contrast, not much is known about the E1BN proteins, apart from the fact that their expression is regulated over the course of infection (Chow et al., 1979; Montell et al., 1984; Sieber and Dobner, 2007; Spector et al., 1978; Takayesu et al., 1994; Virtanen and Pettersson, 1985; Wilson and Darnell, 1981). In a former study we could show first functional data for an E1BN protein by demonstrating, that E1B-156R

* Corresponding author at: Heinrich Pette Institute, Leibniz Institute for Experimental Virology, Department of Molecular Virology, Martinistrasse 52, 20251 Hamburg, Germany. Fax: +49 40 48051 103.
E-mail address: thomas.dobner@hpi.uni-hamburg.de (T. Dobner).
[1] Both authors contributed equally.
[2] Current address: Bruker Biospin AG, 8117 Fallanden, Switzerland.

0042-6822/$ – see front matter © 2011 Elsevier Inc. All rights reserved.
doi:10.1016/j.virol.2011.07.012

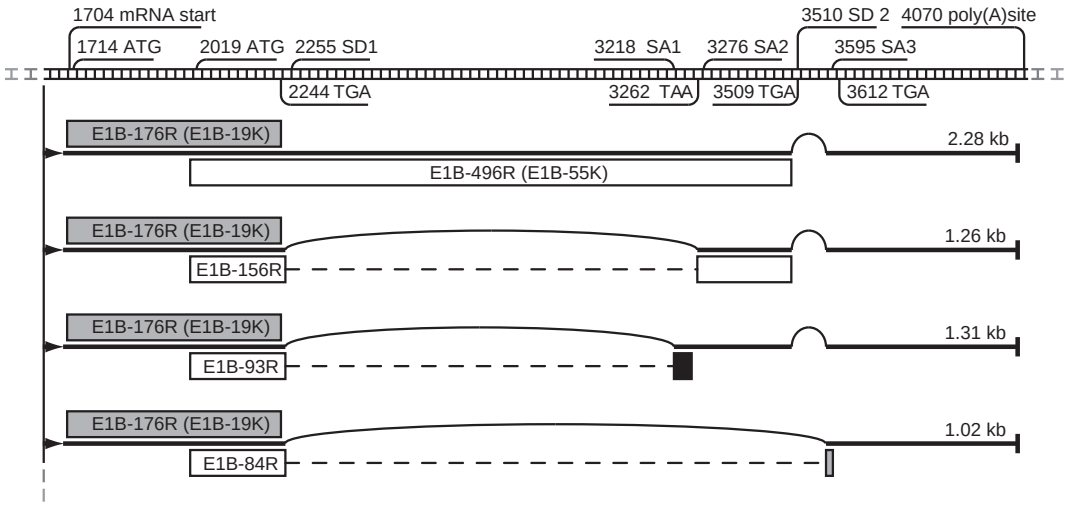

Fig. 1. HAdV5 E1B-region and its gene products. The region and specific landmarks are shown at the top. Numbers refer to nucleotides in the HAdV5 sequence. Four differentially spliced mRNAs are diagrammed below as thick lines. Their length is noted at the right side. Thin printed arcs represent introns between splice donor (SD) and acceptor (SA) sites. The five open reading frames encoding the E1B proteins are illustrated as boxes next to their corresponding mRNA. The shading of the boxes (gray, black and white) depicts the used reading frames 1 to 3. The gene products are termed with correspondence to their number of amino acid residues. E1B-176R and E1B-496R therefore represent E1B-19K and E1B-55K. The open reading frames of E1B-156R, E1B-93R and E1B-84R are generated through fusion of two exons. The eliminated intron sequences are illustrated as dashed lines. This figure was adapted from (Sieber and Dobner, 2007) with permission of ASM. Nucleotide sequence data of the E1BN open reading frames were acquired by us by sequencing cDNAs derived from E1B-mRNAs of infected cells (Sieber and Dobner, 2007) and confirmed existing predictions (Takayesu et al., 1994). They are available in the Third Party Annotation Section of the DDBJ/EMBL/GenBank databases under the accession number TPA: BK008010. Further annotations were derived from the published HAdV5 sequence from GenBank accession no. AY339865.

promotes transformation independent from repression of p53-transactivation. Further we detected that E1B-156R interacts with E4orf6 and the cellular protein Daxx (Sieber and Dobner, 2007).

The fact that four different proteins contain the same characteristic N-terminus is intriguing and suggests that it could mediate important functions and interactions shared by all of these proteins. However, so far no function or interaction could definitely be assigned to this region. In order to lay a foundation for future rational-driven studies to uncover the role of the common E1B N-terminus, we set out to gain information about its structure using E1B-93R as a model.

Here we show by CD and NMR spectroscopic as well as *in silico* analyses that E1B-93R is an intrinsically disordered protein (IDP). The performed studies further indicate that also the common N-terminus within E1B-55K and the other E1BN proteins is likely intrinsically disordered. As intrinsically disordered proteins and regions (IDRs) are often found to mediate multiple protein/protein interactions (Dyson and Wright, 2002; Uversky, 2002), these data underscore the potential importance of this element in regulation and function of E1B-55K and the E1BN proteins. Additionally we made the observation that E1B-93R induces metachromasia in Coomassie Brilliant Blue (CBB) and appears negative in silver nitrate staining. Though both features have already been observed with other proteins, our analyses on E1B-93R and our in-depth review of published data revealed for the first time a stunning link between these extraordinary stainings and intrinsic disorder. As especially metachromasia seems only to be induced by a specific fraction of IDPs, it can be used to define an IDP subclass and thereby improve our understanding of the nature of IDPs.

Results

Computational analysis of E1B-93R structure

Initially an analysis of the primary amino acid sequence of E1B-93R with different protein structure prediction tools was performed. First four separate secondary structure predictions were made. The modern predictors used here achieve high levels of accuracy (SSPro 77% (Cheng et al., 2005); Porter 80% (Pirovano and Heringa, 2010); NetSurfP 81% (Petersen et al., 2009); I-TASSER/PSIPRED 77% (Jones, 1999)). All predictions suggested a mainly unfolded protein with a small content of structured elements. Predominant was an α-helical stretch of 3 to 14 aa within a glycine/alanine-rich region at position 45–61 (Fig. 2A).

To predict the 3D-structure of E1B-93R I-TASSER was used. This predictor uses a multistep protocol and combines threading (comparison with similar proteins of known structure) and *ab initio* (*de novo* buildup of protein folds) modeling techniques. It predicts up to five folding models that are ranked based on structural density of the structure clustering (Zhang, 2008). For all these models a confidence score (*C*-score) in the range from −5 (low confidence) to +2 (high confidence) is given to assess the quality of the prediction. In general, models with a *C*-score of >−1.5 are reasonably likely to have a correct fold (Roy et al., 2010).

For E1B-93R the five predicted folding models indicate that most of the protein is coiled/disordered and that it contains only low levels of structured elements (Fig. 2B). None of the predicted folds achieves a *C*-score exceeding −4.0 indicating that no high-probability model for a specific fold could be generated. On the one hand this is due to the remarkable lack of suitable threading templates which indicates unique characteristics for the E1B-93R sequence and limits the power of I-TASSER. On the other hand this result points to a mainly flexible protein with no defined fold.

As these observations would be characteristic for an IDP, further analysis using four distinct prediction tools (IUPRED, DisPro, PONDR-VLXT and RONN; Fig. 2C) for intrinsic disorder were conducted. All these predictions indicated that E1B-93R is mainly or completely intrinsically disordered. As intrinsic disorder is based on the local primary amino acid sequence, the common N-terminus also found in HAdV5 E1B-55K, E1B-156R and E1B-84R is also predicted to be similarly intrinsically disordered in these proteins (Fig. 3A). Further, a comparative alignment of IUPRED predictions for representatives of each human adenovirus species indicates a high conservation of the intrinsic disorder potential in the E1B-55K N-terminus among human adenoviruses (Fig. 3B).

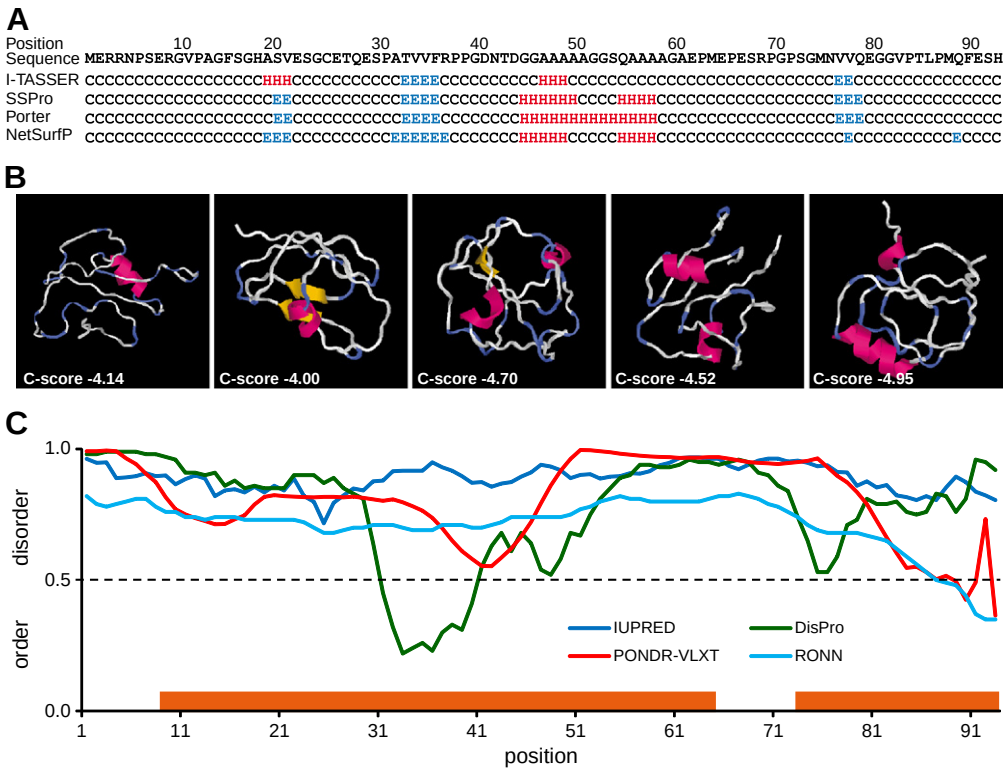

Fig. 2. *In silico* analyses of E1B-93R primary sequence. A. Secondary structure predictions by I-TASSER, SSPro, Porter and NetSurfP. All predictions indicate that E1B-93R is mostly unstructured. The most probable structural element is a helical stretch within the glycine/alanine-rich region at amino acid position 45–61. H: helix, E: strand, C: turn/bend/coil. B. The five E1B-93R 3D-structure models predicted by I-TASSER, ranked by predicted likelihood. The structures are all mainly in coil-formation (gray/blue strings) with little structured (red: helices; yellow: sheets) content. All predictions show a low confidence score (*C*-score), indicating no single high-probability model for a specific fold, but an ensemble of energetically similar interconvertible conformations. C. Prediction of intrinsic disorder by IUPRED, DisPro, PONDR-VLXT and RONN. The predicted degree of disorder tendency (scale 0–1; cutoff 0.5) is charted over the amino acid positions within E1B-93R. All four prediction tools indicate a mostly (DisPro, PONRR VL-XT and RONN) or completely (IUPRED) intrinsically disordered protein structure. Orange bars at the bottom of the diagram indicate the positions of disordered binding domains predicted by ANCHOR.

The prediction of intrinsic disorder based on the primary amino acid sequence is of good accuracy. In a study with PONDR-VLXT (>900 non-homologous proteins), prediction of IDRs with 40 or more residues gave less than 6% false positives (Dunker et al., 2002). The fact that the same set of *in silico* analyses performed for the ordered fibre knob domain of HAdV5 (RCSB Protein data bank file 1KNB) strongly reflects its actual structure (see Suppl. Fig. 1) emphasizes the quality and applicability of these computational tools in this study. To biophysically confirm the structural predictions for E1B-93R, the protein was expressed, purified and analyzed by different, independent techniques.

Expression, purification and identification of E1B-93R

E1B-93R was expressed in *Escherichia coli* as a GST-fusion protein. Subsequent affinity purification was performed using glutathione sepharose. The N-terminal GST-tag was then removed by proteolytic thrombin cleavage while being associated with the affinity matrix. Further application of gel filtration chromatography under native sample conditions allowed the purification of E1B-93R to near homogeneity. The protein was detected by SDS-PAGE and Western blot analysis as it is not detectable by UV absorption, due to its amino acid composition (theoretical extinction coefficient of 0 at 280 nm) (Gill and von Hippel, 1989). The performed immunodetection with the E1B N-terminal specific antibody 2A6 and a sequential Edman degradation of the N-terminal sequence (residues 1–10; Performed by E. Hochmuth, Department of Biochemistry I, University of Regensburg; data not shown) confirmed the identity of the protein as E1B-93R.

E1B-93R shows aberrant mobility in SDS-PAGE

Although E1B-93R has a theoretical molecular mass of 9449.2 Da (including the two additional residues from the thrombin cleavage site) it migrates in SDS-PAGE like a globular protein of about 16 kDa (Fig. 4A). This aberrant migration of E1B-93R has already been observed by others in lysates from transfected or infected cells and is also a known hallmark of IDPs (Lewis and Anderson, 1987; Receveur-Brechot et al., 2006; Sieber and Dobner, 2007; Takayesu et al., 1994).

To confirm that this behavior is not caused by a covalent interaction with another protein ESI mass spectrometry was performed (E. Hochmuth, Department of Biochemistry I, University of Regensburg). Here the purified E1B-93R shows a single peak correlating to a mass of 9757.4 Da (Fig. 4B). This value indicates that the aberrant mobility in the SDS-PAGE cannot be explained by a covalent interaction with itself or another large factor, though smaller modifications cannot be excluded.

Characteristics of E1B-93R in CBB and silver staining

E1B-93R exhibits a non-classical behavior in CBB R-250 and silver nitrate staining. When partially purified GST-E1B-93R was subjected to a 16 h thrombin cleavage and investigated by CBB R-250 staining, the protein band corresponding to E1B-93R appeared pink instead of the normal blue (Fig. 4A lanes 1 to 4 and 6). This so-called metachromasia (Micko and Schlaepfer, 1978; Hattori et al., 1996) was reproducibly seen for E1B-93R but not for GST. When protein samples were used in silver nitrate staining the E1B-93R band (Fig. 4A

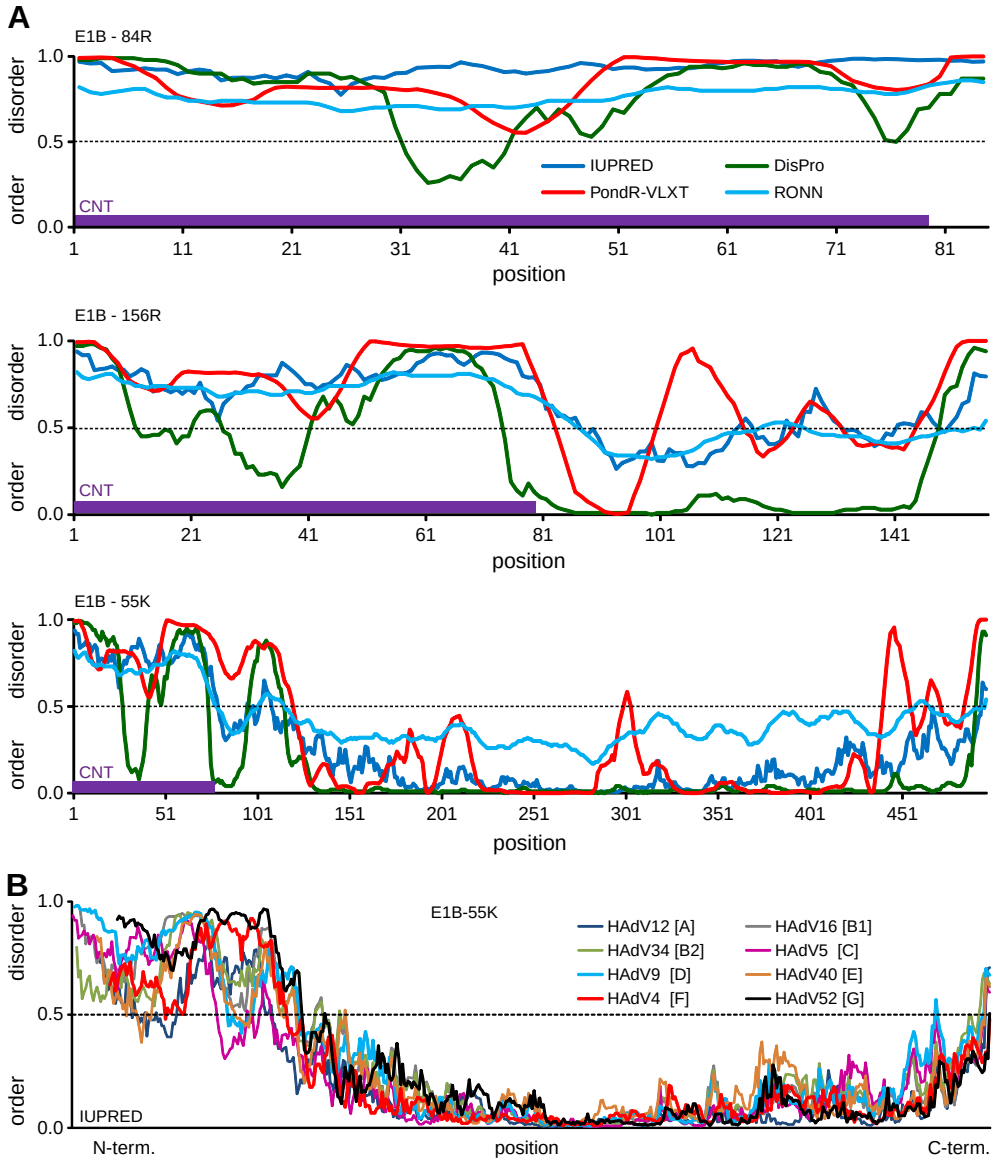

Fig. 3. Intrinsic disorder in E1B N-terminus. A. Prediction of intrinsic disorder in E1B-84R, -156R and -55K by IUPRED, DisPro, PONDR-VLXT and RONN. The legend found in the diagram of E1B-84R applies to all three proteins. The predicted degree of disorder tendency (scale 0–1; cut off 0.5) is charted over the amino acid positions of the proteins. All four prediction tools indicate a high level of intrinsic disorder in the common N-terminus of all investigated proteins. The expanse of the common N-terminus (CNT) is indicated as a violet bar at the bottom of each diagram. B. Order/disorder predictions for E1B-55K proteins of representatives of all human adenovirus species (A, B1, B2, C-G) by IUPRED web server. All predictions are very similar and show intrinsic disorder in the N-terminus. As especially the N-termini differ in length, all protein sequences were aligned to their C-terminal end, causing the starting point of the individual graphs to shift slightly.

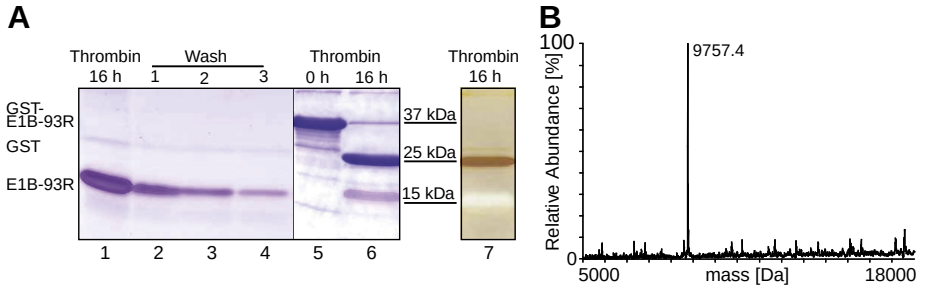

Fig. 4. Electrophoretic mobility, staining behavior and mass of E1B-93R. *A.* Aberrant electrophoretic mobility (16 kDa) and coloration of E1B-93R in stained SDS-PAGE gels. Serial dilution of E1B-93R deriving from GST-E1B-93R, which was first bound to *Glutathione Sepharose™ 4B* matrix (Amersham) and then treated with thrombin for 16 h to release E1B-93R. Aliquots from the thrombin treated sample (lane 1) and from subsequent PBS-washing steps (lanes 2 to 4) were separated on SDS-PAGE and stained with CBB R-250. In a second experiment 80 µg of partially purified GST-E1B-93R were separated on SDS-PAGE directly (lane 5) or after 16 h thrombin cleavage (lanes 6 and 7) and CBB R-250 (lane 5 and 6) or silver stained (lane 7). On the left the proteins corresponding to the different bands are marked. Between lanes 6 and 7 relevant molecular mass marker bands are depicted. *B.* Mass spectrometric analysis of E1B-93R. These data show that E1B-93R has an electrophoretic mobility expected for a 16 kDa protein (A) while its mass was determined to be 9757.4 Da (B). Further the protein shows a characteristic staining with CBB (reddish instead of blue) and in silver nitrate staining (negative band) (A).

lane 7) appeared negative (lighter stained than background). This effect cannot be due to an "overload" of protein, which might lead to a band with a bleached out center, as the equimolar GST-band showed the classical yellow/brown color under the same conditions (Rabilloud et al., 1994).

Determination of E1B-93R concentration

To evaluate the concentration of purified E1B-93R Bradford (Bradford, 1976) and bicinchoninic acid protein assays (BCA Assay, Sigma) were performed. The Bradford assay gave negative concentration values (data not shown). As this assay is based on CBB G-250, the effect is likely caused by the same mechanism as the observed metachromasia. The BCA assay in contrast gave reasonable values. Though, it has to be noted that the accuracy of the measured values might also be affected by the predicted intrinsically disordered nature of E1B-93R, as it was shown that concentrations of IDPs can often be largely and unpredictably underestimated by all standard assays (e. g. Bradford assay, BCA assay, comparison to a known reference in SDS-PAGE and UV-absorption) (Szollosi et al., 2007). The concentrations given here are therefore intended only for a direct comparison among each other.

Analyses of E1B-93R structure by CD and NMR spectroscopy

The successful purification of HAdV5 E1B-93R allowed the elucidation of its secondary structure composition using CD and NMR spectroscopy. The CD spectroscopic analysis of purified HAdV E1B-93R (Fig. 5) performed at room temperature revealed a major peak at about 198 nm, which is typical for a polypeptide in random-coil conformation (Boulant et al., 2005). Negative ellipticity values at 212–245 nm further indicate the presence of residual ordered secondary structures. A more detailed analysis of the secondary structure content though is not feasible without knowledge of the precise E1B-93R concentration (see above).

In order to consolidate these CD spectroscopic data the purified E1B-93R protein was further analyzed using NMR spectroscopy. Here, the 1D NMR ^{1}H-spectrum of 1 mM E1B-93R recorded at a frequency of 600 MHz (Fig. 6A) also identified the adenoviral protein as being mainly unfolded by a lack of characteristic resonances of β-strand NH- (>9 ppm) and H^{α}-protons (≈4.8–5.9 ppm) as well as typical high field shifted resonances of hydrophobic core CH_3-protons (<0.8 ppm). The obtained 1D-spectrum is typical for an unfolded protein with a spectrum consisting of a superposition of resonance lines at the known random-coil positions (see e. g. (Arnold et al., 2002)). The resonances of methyl groups of the thirteen alanine residues can be identified at 1.40 ppm, the H^{γ}-resonances of the seven valine residues and the H^{δ} of the leucine residue can be detected between 0.89 and 0.94 ppm. The same is true for other resonances as the ring resonances of the two histidine and the three phenylalanine residues. Using the DSS (2,2-dimethyl-2-silapentane-5-sulfonaic acid)-signal as internal standard, the integration of methyl peaks of the alanine residues allows an estimation of protein concentration. The concentration obtained for the used sample corresponds within the limits of error to the value determined by BCA assay. Random-coil spectra can also be obtained from protein aggregates where only a small part of the protein is mobile but the other part is not visible in the NMR-spectra. Therefore the analysis also excludes an unspecific aggregation of E1B-93R since the majority of all resonances is visible as it should be the case for a predominantly disordered, but not aggregated protein. In addition to confirming of the CD spectroscopy data, these results also correspond with results from ^{1}H,^{1}H TOCSY (total correlation spectroscopy) and NOESY (nuclear Overhauser effect spectroscopy) experiments showing the protein's coil conformation, a minor α-helical folded region and no signals indicating β-sheet (Fig. 6B). Furthermore the very small spread of resonance frequencies for amide protons together with the scarcity of nuclear Overhauser effects in the NH-NH-region are typical for a protein without significant stable secondary structure (Habchi et al., 2010; Karlin et al., 2002; Longhi et al., 2003) (Fig. 6B).

To yield more detailed information about the protein's conformational properties and its local backbone mobility, respectively, the ^{1}H,^{15}N NOE values were measured at a E1B-93R concentration of 1 mM for 83 backbone amide nitrogen atoms of E1B-93R. As expected, the majority of residues exhibit reduced ^{1}H,^{15}N NOE values (<0.4) which is indicative for the high conformational flexibility of a mainly unstructured protein (Mayor et al., 2003; Sam et al., 2002; Wojciak et al., 2002). In contrast to that, approximately 13 residues of E1B-93R (≈14%) appeared to be relatively ordered as they showed slightly elevated ^{1}H,^{15}N NOE values (Fig. 6C). Three of these signals are found in the range associated with typical chemical shifts of glycine residue cross peaks in disordered proteins (indicated in Figs. 6C and D) (Tamiola et al., 2010; Wang and Jardetzky, 2002). As the chemical shift ranges for other amino acids are not so well separated, a clear association of the remaining 10 signals with NOE values>0.4 is difficult. But, since the most dominantly predicted α-helical region (Fig. 2A; around residue 51) is alanine-rich, the approximate chemical shift range for alanines is also highlighted (Figs. 6C and D) (Tamiola et al., 2010; Wang and Jardetzky, 2002). In

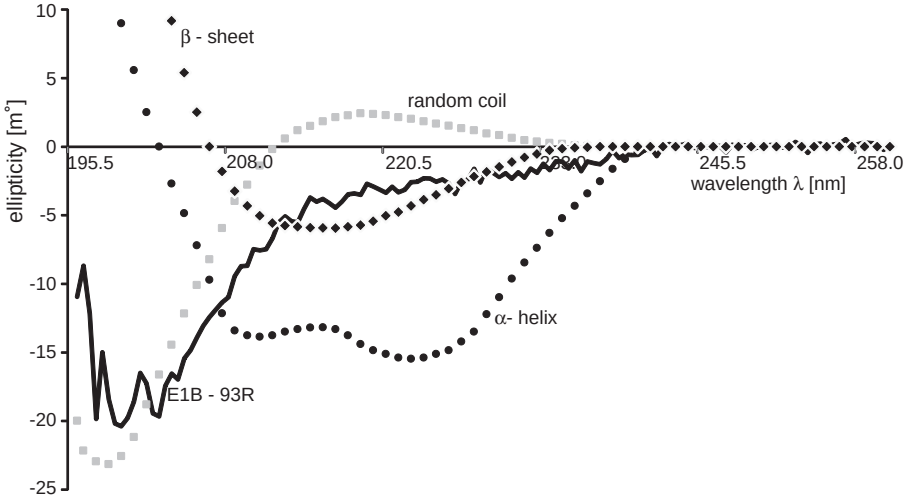

Fig. 5. Circular dichroism spectrum of E1B-93R. Shown is the PBS-baseline corrected average ellipticity ($n=3$) of E1B-93R (black line) over a wavelength range of 195.5 to 260.0 nm (path length 1 mm; 0.5 nm step resolution; 5.5 nm/min scanning speed; room temperature) in m°. Further, the scale free theoretical spectra of pure α-helix (black circles), β-sheet (black diamonds) and random coil (grey diamonds) are given based on (Johnson, 1990). The spectrum of E1B-93R corresponds best with that of pure random coil, but negative ellipticity values at 212–245 nm indicate residual structured elements.

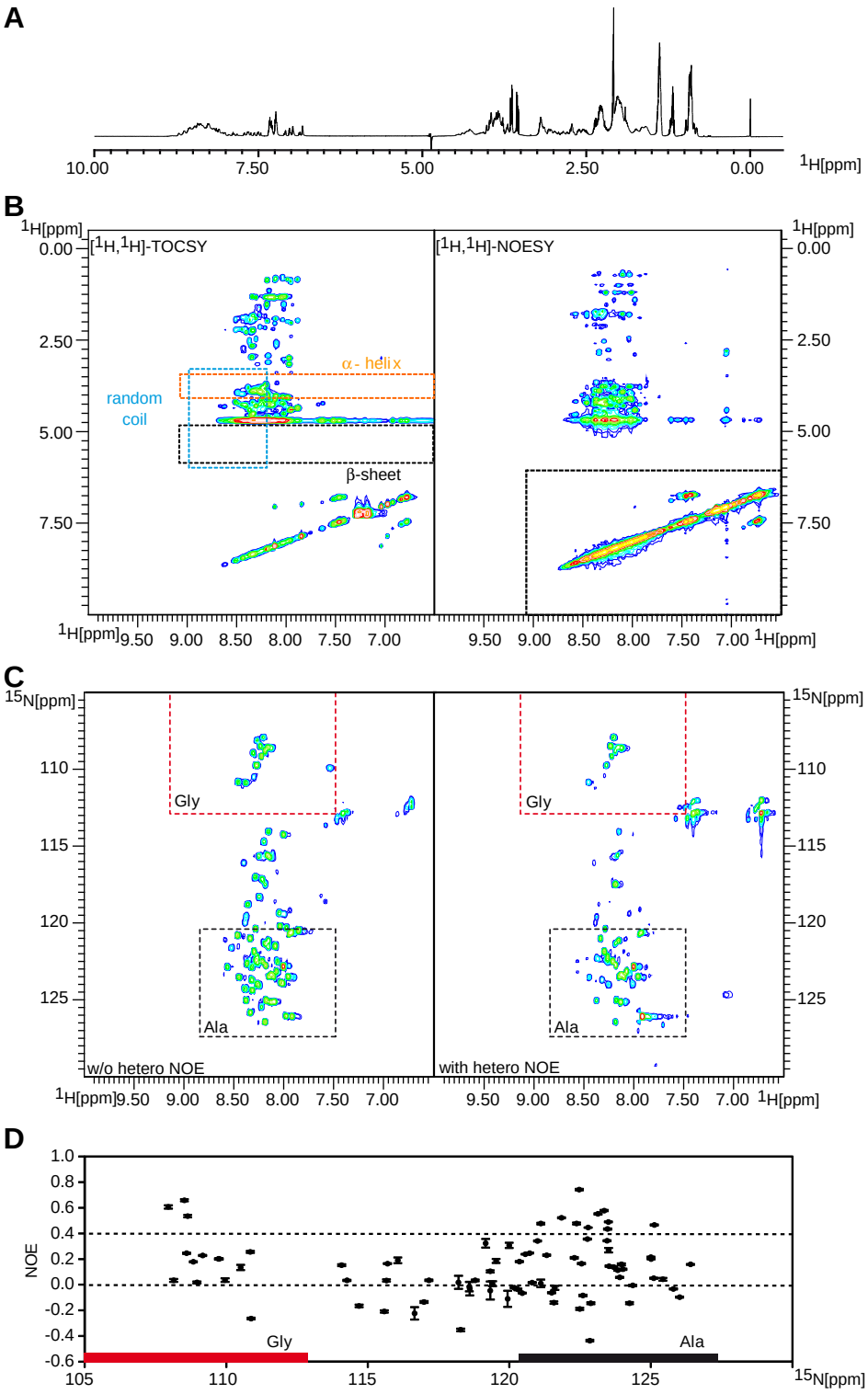

Fig. 6. NMR-spectra of E1B-93R. A. 1D ^{1}H NMR-spectrum of E1B-93R. B. 2D ^{1}H,^{1}H TOCSY- and NOESY-spectra. In the TOCSY-spectrum (left) characteristic fingerprint regions for α-helix (orange; 3.40–4.10 ppm), β-sheet (black; 4.85–5.90 ppm) and random coil (blue; 8.20-9.00 ppm) are highlighted (Wishart et al., 1991). In the NOESY-spectrum (right) the region containing possible inter-residual NH-NH-cross signals is marked by a dashed box. C. 2D ^{1}H,^{15}N NMR-spectra without (left) and with (right) hetero NOE. Chemical shift ranges expected for glycine (red; 8.31 ± 0.83 ppm; 108.8 ± 4.1 ppm) and alanine (black; 8.16 ± 0.68 ppm, 123.9 ± 3.5 ppm) residues in unstructured polypeptides are indicated with standard deviations (Tamiola et al., 2010; Wang and Jardetzky, 2002). Only positive cross peaks are shown. D. Intramolecular flexibility of amino acid residues. ^{1}H,^{15}N NOEs of 83 identifiable NH-protons are shown with standard deviation. Cross peaks were ordered according to ^{15}N chemical shifts. The ^{15}N shift range of glycine (red) and alanine (black) residues in disordered proteins are indicated as bars at the bottom of the diagram (Tamiola et al., 2010; Wang and Jardetzky, 2002). NOE values "0.0" and "0.4" are indicated by dashed lines. These NMR analyses indicate that E1B-93R is mostly unstructured and overall highly flexible. The protein contains some structured elements – probably of α-helical nature – that could consist of glycines and alanines.

fact, all remaining 10 residues with NOEs indicative for some residual structure fall into this range.

Taken together, the structural analysis of E1B-93R revealed that E1B-93R is an overall intrinsically disordered protein with a small ordered region of about 14% most likely representing an α-helical folding.

Discussion

E1B-93R is an IDP

It was a long standing belief that a protein has to attain a stably folded conformation to perform its physiological functions. However in the last decade it became clear that many functional proteins contain large unfolded regions or are lacking a defined secondary and tertiary structure altogether (Romero et al., 1998). In fact, there is evidence that considerable numbers of unfolded proteins or regions are found in all living organisms and that they perform essential cellular functions (Tompa, 2002). Due to their high flexibility IDPs can provide large interaction surfaces and mediate interactions with high association/dissociation rates. Often IDPs/IDRs interact with multiple partners and acquire defined folds that are specific for the individual interactions (Dyson and Wright, 2002; Uversky, 2002). Due to this, intrinsic disorder is often found in proteins that act as hubs in interaction networks involved in regulatory and signaling events. Here their specific nature enables them to form high-specificity, low-affinity interactions with many structurally distinct partners (summarized in (Uversky, 2009)).

Our computational analyses predict a high level of intrinsic disorder in E1B-93R. The data from CD spectroscopy and different NMR techniques confirm this and indicate that E1B-93R is mostly unstructured, highly flexible and lacking a hydrophobic core. These data show together with other intrinsic features of the protein (aberrant mobility in the SDS-PAGE, characteristic amino acid composition, etc.) that E1B-93R is indeed an IDP (summarized in Table 1).

NMR and CD data indicate further only low levels of secondary structure, namely an α-helical content of about 14% (≈13 residues). This observation does not contradict with the fact that E1B-93R is an IDP, as even highly disordered proteins may still contain residual amounts of secondary structures (Galea et al., 2008; Peng et al., 2005). As IDPs exist as a dynamic ensemble of different structures, the observed secondary structure content might be caused by an element conserved in most or all of the possible states of the ensemble. The likeliest candidate – even though it was not recognized as ordered (Fig. 2C) – is located within the glycine/alanine-rich stretch (residues 45–61), as it contains the only α-helical element predicted by the consensus of the secondary structure predictions (Fig. 2A). In concert with this, all 13 signals with elevated ^{1}H,^{15}N NOEs (>0.4) are found in the chemical shift range typical for glycine and alanine residues (3 and 10 residues, respectively) (Tamiola et al., 2010; Wang and Jardetzky, 2002) and therefore fit well to the primary sequence of the presumed element.

The findings on E1B-93R correspond well to the observation that many viruses make extensive use of intrinsic disorder (Xue et al., 2010). Further, it is already known that two human adenovirus proteins, the DNA-binding protein (Dekker et al., 1998; Dunker et al., 2002; Tucker et al., 1994; van Breukelen et al., 2000) and E1A (Ferreon et al., 2009; Pelka et al., 2008), are at least partially disordered. The enrichment in viruses is believed to be caused, at least in part, by the need for economic use of a limited genome (Xue et al., 2010). Intrinsic disorder seems to support this need, as it not only correlates with multifunctionality, but also with expression from overlapping and/or alternatively spliced reading frames (Kovacs et al., 2010; Rancurel et al., 2009; Romero et al., 2006), a setup also used in the E1B transcription unit (Fig. 1).

Table 1
Comparison of features of intrinsically disordered proteins and E1B-93R.

Common features of IDPs	E1B-93R
Depleted in V, L, I, F, W, Y, C, N	16.1% (average frequency[a]: 36.2%)
Enriched in Q, S, P, E, K, R, G, A	68.8% (average frequency[a]: 47.4%)
Often proline rich	11.8% (average frequency[a]: 4.6%)
Often glycine rich	15.1% (average frequency[a]: 8.0%)
Low absorbance at 280 nm	theoretical value = 0
Little secondary structure	about 14% α-helix
High flexibility	high flexibility
Hypervariable in sequence	N-terminus is least conserved region in E1B-55K
Reduced mobility in SDS-PAGE	expected: 9.3 kDa[b]; observed 16 kDa

Known hallmarks of intrinsically disordered proteins (as summarized in (Receveur-Brechot et al., 2006; Uversky, 2009)) (left) are reflected in the corresponding characteristics of E1B-93R (right).

[a] Average frequency of the stated amino acids within globular proteins is given in comparison (Tompa, 2002).

[b] Theoretical molecular weight computed by ProtParam at ExPASy proteomics serve.

E1B-93R properties help to define a new IDP subclass

We could show that E1B-93R is an IDP, but its negative silver staining and its extraordinary behavior in interaction with CBB help to further characterize the protein (Fig. 4A). There exists a multitude of silver staining techniques that differ in sensitivity and specificity (e. g. (Chevallet et al., 2006; Friedman, 1982; Rabilloud, 1990)), though the basic principle is always the same: proteins complex silver ions that are subsequently reduced to form visual deposits of elemental silver. The staining is therefore mostly dependent on the amount of bound ions and the strength of their complexation, as a strong interaction inhibits the reduction. A negative band therefore can be formed, if a very low amount of silver ions (in comparison to the surrounding protein-free gel matrix) is bound and/or the ions are strongly complexed (resumed by (Rabilloud, 1990)). Such negative staining is rare, but known for some human salivary proteins (Beeley et al., 1996; Marshall, 1984), conalbumin (Morrissey, 1981), pepsin (Tal et al., 1985; Yüksel and Gracy, 1985), histone H1 (Nielsen and Brown, 1984) and other factors (Plowman et al., 2000; Zhou and Wolk, 2002). As it was claimed that the silver stainability of proteins is determined by their "structural features" rather than individual amino acids (Gersten et al., 1991), it is tempting to speculate that intrinsic disorder might be the causative factor for negative staining. Such a general link though cannot be established, as the effect is observed for ordered (pepsin (Cooper et al., 1990)) as well as disordered proteins (E1B-93R and histone H1 (Nielsen and Brown, 1984; Vila et al., 2000, 2001). But as different settings can induce negative bands (e. g. little ion binding and/or strong complexation), it seems that at least one such setting is fulfilled by a specific fraction of IDPs, that includes H1 and E1B-93R.

One effect that might contribute to negative staining of IDPs is linked to their reduced mobility in SDS-PAGE, which is caused by reduced SDS binding and thereby a lower density of negative charges on the protein (Tompa, 2002). As the negative charges of SDS are also believed to tether silver ions to proteins, the same effect might actually reduce the amount of complexed ions (Rabilloud, 1990) and therefore diminish the staining of IDPs.

Another extraordinary feature of E1B-93R is the fact that it appears pink in CBB staining of SDS-PAGE gels instead of the classical blue coloration. This metachromasia has been described for a limited set of proteins, namely collagen (McCormick et al., 1979; Micko and Schlaepfer, 1978), histone H1 (see Suppl. Fig. 2), H2B (Duhamel et al., 1980), H5 (Duhamel and Brendel, 1983), and parotid proline-rich proteins (Bedi and Bedi, 1995; Beeley et al., 1996; Shatzman and Henkin, 1983). The underlying functional basis was claimed to be a strong underrepresentation of hydrophobic amino acids that affects the electronic transition of the bound dye and thereby induces the discoloration (Hattori et al., 1996). As a depletion of hydrophobic residues is also a hallmark of intrinsic disorder (Dunker et al., 2001), we assume that both features might be connected on the level of primary

protein structure. This model is heavily supported by the strong correlation between metachromasia associated proteins and intrinsic disorder. H1.0 (Vila et al., 2000, 2001), H5 (Graziano et al., 1990) and also a basic salivary proline-rich protein (parotid o protein) (Loomis et al., 1985) have already been described to be mostly intrinsically disordered. Further, monomeric H2B was claimed to be an IDP and recently shown to have only a limited secondary structure contend of 31% (Stump and Gloss, 2008; Uversky et al., 2000). Also monomeric collagen is considered an IDP (Uversky et al., 2000) and shows the indicative aberrant mobility in SDS-PAGE (Hayashi and Nagai, 1980). The observation that similar to E1B-93R also collagen and histone H1 (Duhamel et al., 1981; Hattori et al., 1996) cannot be readily quantified by the CBB-based Bradford assay, further supports the proposed relationship.

Though induction of metachromasia seems to be indicative for intrinsic disorder, the opposite is not valid for all IDPs, as many do not show obvious metachromasia (personal correspondence P. Tompa; Institute of Enzymology, Hungarian Academy of Sciences, Budapest, Hungary). It has further been shown that while concentrations of IDPs are often underestimated in Bradford assay the scope of error varies widely among different proteins (Szollosi et al., 2007). We therefore suggest that induction of metachromasia is specific for a subclass of IDPs and that this can be used in the ongoing attempt of the field to subdivide IDPs into more distinguishable subclasses or "flavors" (Linding et al., 2003; Vucetic et al., 2003). Further, the discovered connection to intrinsic disorder might represent an answer to the question concerning the structural basis of metachromasia — a question that has been discussed for more than 30 years (Micko and Schlaepfer, 1978).

Intrinsic disorder in the common N-terminus of E1B-55K and the E1BN proteins

The data collected here for E1B-93R can also be used to expand our knowledge on E1B-55K and the other E1BN proteins due to the fact that E1B-93R mainly consists of the common N-terminus, which is also found in these proteins. As intrinsic disorder is defined by local amino acid composition, the common N-terminus mandatorily has comparable disorder potential in all of these proteins, which is also reflected by the results of order/disorder predictions (Fig. 3A). Another supporting fact is the observation that the N-terminus is the least conserved region of E1B-55K (Kindsmuller et al., 2009) and as intrinsically disordered regions are on average much more variable than ordered domains, such hypervariability is valued as an indicator for disorder (Brown et al., 2002). Consistently, order/disorder analyses indicate that though the sequence is variable, the intrinsic disorder potential in the N-terminus is highly conserved among representatives of all human adenovirus species (Fig. 3B). These considerations strongly indicate that the common N-terminus represents an IDR.

The IDR in the common N-terminus is a likely candidate interaction site

As IDRs often mediate multiple protein/protein interactions (Dunker et al., 2005), the knowledge that the common N-terminus is such a region identifies it as a likely candidate site for binding of interactors. Further *in silico* analysis (ANCHOR; (Dosztanyi et al., 2009)) of the N-terminus supports this idea, as it indicates that a large part of the region is a disordered binding region (Fig. 2C; residues 8 to 64). Such regions undergo disorder-to-order transition upon binding of globular interaction partners (Dyson and Wright, 2002; Uversky, 2002) and are predicted by a highly disordered sequential neighborhood, unfavorable interchain energies and more favorable interaction energies with a globular partner (Dosztanyi et al., 2009).

This study therefore can be used to focus the respective investigations to identify interaction sites to this region. In fact, there are already several cellular and viral proteins known to interact with the E1B-55K at yet unknown sites. Among these factors are cellular PML V (Wimmer et al., 2010), SSBP2 (Fleisig et al., 2007), WT1 (Maheswaran et al., 1998), and DNA Ligase IV (Baker et al., 2007) as well as adenoviral E4orf3 (protein encoded by early transcription unit 4 open reading frame 3) (Leppard and Everett, 1999). Further we could recently show that E1B-156R interacts with p53 and E4orf6 (Sieber and Dobner, 2007). As these two proteins are also supposed to bind to the central part of E1B-55K (Rubenwolf et al., 1997; Yew and Berk, 1992), which is not found in E1B-156R, additional sites sufficient for interaction must exist either in the C-terminus of E1B-156R or within the common N-terminus.

In conclusion, our studies do not only show that E1B-93R is a defining member of a specific IDP subclass, but also suggest that the N-terminus common to E1B-55K and all E1BN proteins is an IDR with potential to mediate important interactions.

Materials and methods

Plasmid pGEX-2T-E1B-93R

The cDNA of E1B-93R was acquired from cytoplasmic mRNA of H5*dl*309 (Jones and Shenk, 1979) infected HeLa cells (Gey et al., 1952) by reverse transcription with oligo (dT) primers. The coding sequence was gained by PCR from these cDNAs and inserted between the *BamHI* and *EcoRI* sites of the expression vector pGEX-2 T (Pharmacia). The resulting plasmid encodes an N-terminally GST-tagged E1B-93R protein (GST-E1B-93R) with a thrombin cleavage site ("/") in its six amino acid linker (L V P R/G S).

Expression and purification of E1B-93R

E. coli TOPP™3 (Stratagene) transformed with pGEX-2T-E1B-93R were grown at 37 °C in Lysogeny Broth (LB) medium ($c_{Ampicillin} = 0.1$ g/l) for production of unlabeled protein (Bertani, 1951; Bertani, 2004). At an optical density (wavelength: 600 nm) of 0.6–0.8 protein expression was induced with 0.5 mM isopropyl-β-D-thiogalactopyranoside for 5 h at 30 °C. Bacteria were then harvested by centrifugation and suspended in 20 ml PBS. After addition of 7.5 mg lysozyme, 10 μg/ml DNase I, 13 mM $MgCl_2$, 1.3 mM $MnCl_2$ and 10 min incubation on ice the cells were sonicated (output 8; 80% duty cycle; 5 times; 1 min; 4 °C, Branson Sonifier 450). NaCl and Triton-X-100 were added to a final concentration of 0.5 M and 1%, respectively. The suspension was incubated on ice for 10 min and centrifuged (14,500*g*; 45 min; 4 °C). The supernatant was incubated with 1 ml equilibrated (washed three times in PBS (pH 7.1–7.2) and once in PBS with 0.5 M NaCl and 1% Triton-X-100) *Glutathione Sepharose™ 4B* matrix (Amersham) for 1 h at 4 °C while gently agitating. The resin was washed twice (10 ml PBS (pH 7.1–7.2) with 1% Triton-X-100 and 10 ml PBS; 500 g; 5 min; 4 °C). For structural studies the matrix-associated fusion protein was cleaved with thrombin (50 U/ml matrix, Amersham) in PBS (16 h at 22 °C) and eluted four times with 1.5 ml PBS each. Samples shown in Fig. 4 lanes 5 and 6 were eluated (150 mM NaCl, 50 mM Tris, 50 mM glutathione) and dialyzed. The sample in lane 6 was then treated with thrombin (2 U per mg protein; 16 h; 22 °C; gentle agitation). The eluted E1B-93R was further purified by gel filtration chromatography (Äkta FPLC, Amersham Pharmacia Bioscience). The gel filtration was performed in sterile filtered PBS buffer (flow rate = 1.5 ml/min) at 4 °C using a *HiLoad™ 16/60 Superdex™200* column (Amersham). The eluted fractions were analyzed by SDS-PAGE followed by Western blot analysis (Marton et al., 1990) with antibody 2A6 (Sarnow et al., 1982) or CBB R-250 staining (see below). E1B-93R containing fractions were pooled. DTT and EDTA were added to final concentrations of 5 mM and 0.5 mM, respectively. Finally, samples were concentrated (Vivaspin 2 ml concentrators; molecular weight cut off = 3 kDa, Vivascience). Concentrations were estimated by Bradford (Bradford, 1976) or Bicinchoninic Acid Protein assay (BCA assay, Sigma).

CBB R-250 staining

SDS-PAGE gels were stained with 0.1% CBB R-250 (Merck) in acetic acid:ethanol:water (10:40:50) for 25 min and then destained with acetic acid:ethanol:water (10:45:45).

Silver nitrate staining

SDS-PAGE gels were fixed for 30 min in an acetic acid:ethanol: water (15:30:55) mixture and sensitized for 10 min (4.1% sodium acetate and 0.2% sodium thiosulfate pentahydrate in a 25:75 ethanol: water mixture). After washing three times 5 min in water the gel was incubated for 10 min in the silver nitrate solution (0.1% silver nitrate and 0.025% formaldehyde in water). After washing three times 20 sec with water, the gels were developed (2.5% disodium carbonate and 0.019% formaldehyde in water; pH 11.5). The reaction was stopped by 1.86% EDTA in water. All incubation steps were performed at room temperature under mild agitation. Gels were stored in water.

ESI Mass spectrometry

Mass spectrometry was performed by E. Hochmuth, Department of Biochemistry I, University of Regensburg. 500 pmol of purified protein were subjected to a 20 min gradual buffer exchange (7–70% actonitril/ TFA buffer) on a reversed phase C4-column. E1B-93R in 70% acetonitril/0.05% TFA buffer (pH 2) was measured at room temperature with a SSQ 7000 Finigan MAT.

Circular dichroism spectroscopy (CD)

Circular dichroism spectra were recorded over a wavelength range of 195.5–260 nm using an Aviv 62-DS spectropolarimeter (Aviv Associates). Purified E1B-93R at a measured concentration of 7 μM in PBS (according to BCA assay) was analyzed in a quartz cuvette.

NMR data collection and analysis

Purified HAdV5 E1B-93R protein was prepared to a final concentration of 1 to 1.57 mM (according to BCA assay) in PBS (pH 7.1–7.2) supplemented with 5% D_2O, 1% protease-inhibitor cocktail (Sigma) and 0.1 mM of 2,2-dimethyl-2-silapentane-5-sulfonaic acid (DSS) as an internal reference. For heteronuclear experiments uniformly ^{15}N enriched protein was produced by growing the bacteria in a modified new minimal medium (Budisa et al., 1995) supplemented with 1 g/l (^{15}N, 99%)-NH_4Cl and 0.1 g/l ampicillin, as described by Gronwald et al. (Gronwald et al., 2001). All NMR experiments were recorded at 293 K on Bruker AVANCE 500 and 600 spectrometers operating at proton resonance frequencies of 500.13 MHz and 600.13 MHz, respectively. ^1H chemical shifts were referenced to DSS used as internal standard. ^{15}N chemical shifts were indirectly referenced to DSS as described by Wishard et al. (Wishart et al., 1995). 1D ^1H-spectra were recorded on 1 mM E1B-93R in PBS (pH 7.1–7.2) with 5% D_2O (600.13 MHz; 293 K; 16 scans; program: zggpw5). Sensitivity enhanced ^1H,^{15}N heteronuclear single quantum coherence experiments were recorded with 2048×1024 complex data points using a sweep width of 14 ppm in the ^1H dimension and 40 ppm in the ^{15}N dimension. 2D ^1H,^{15}N NMR-spectra with and without hetero NOE were measured with 1 mM ^{15}N isotopically labeled E1B-93R in PBS (pH 7.1–7.2) with 5% D_2O at 293 K (128 scans; program: hsqcnoef3gpsi). Heteronuclear ^1H,^{15}N NOEs were attained according to Farrow et al. (Farrow et al., 1994). Homonuclear 2D ^1H,^1H NOESY- and ^1H,^1H TOCSY-spectra were recorded with samples of 1.57 mM E1B-93R in PBS (pH 7.1–7.2) with 5% D_2O at 293 K (600.13 MHz; 32 scans; program: noesygpph19; 100 ms mixing and 500.13 MHz; 32 scans; program: mlevgpph19; 60 ms mixing, respectively). Topspin 1.1 (Bruker Biospin) and Auremol (Gronwald and Kalbitzer, 2004) were used to process and analyze the data.

Computational analyses

3D protein structures were predicted by I-TASSER (http://zhanglab.ccmb.med.umich.edu/I-TASSER/) (Roy, Kucukural, and Zhang; Zhang, 2007; Zhang, 2008). Pairwise alignments of 3D structures were performed by FATCAT (http://fatcat.burnham.org/fatcat/) (Ye and Godzik, 2003). For prediction of intrinsic disorder the services of IUPRED (www.iupred.enzim.hu) (Dosztanyi et al., 2005a,b), PONDR-VLXT (www.pondr.com; [*access to PONDR was provided by Molecular Kinetics, 6201 La Pas Trail-Ste 160, Indianapolis, IN 46268; 317-280-8737; main@molecularkinetics.com; PONDR is copyright©2004 by Molecular Kinetics, all rights reserved*]) (Peng et al., 2005), DISpro (http://scratch.proteomics.ics.uci.edu/) (Cheng et al., 2005) and RONN (http://www.strubi.ox.ac.uk/RONN) (Yang et al., 2005) were utilized. Secondary structure predictions were performed by SSPro (http://scratch.proteomics.ics.uci.edu) (Cheng et al., 2005), Porter (http://distill.ucd.ie/porter/), NetSurfP (Petersen et al., 2009) (http://www.cbs.dtu.dk/services/NetSurfP/) and I-TASSER (uses PSI-PRED) web servers. Theoretical molecular weight was estimated with ProtParam at ExPASy Proteomics Server (http://www.expasy.ch/cgi-bin/protparam). Disordered binding regions were predicted by ANCHOR (http://anchor.enzim.hu/) (Dosztanyi et al., 2009).

Supplementary materials related to this article can be found online at doi:10.1016/j.virol.2011.07.012.

Acknowledgements

We thank Barbara Härtl, Klaus Tiefenbach, Roland Hofweber, Eduard Hochmuth and Helmut Durchschlag for assistance and help. We further thank Peter Tompa for information on staining behavior of different IDPs and fruitful discussion. This work was supported by the Wilhelm-Sander-Stiftung, Munich, Germany. The Heinrich Pette Institute is supported by the Freie und Hansestadt Hamburg and the Bundesministerium für Gesundheit.

References

Anderson, C.W., Schmitt, R.C., Smart, J.E., Lewis, J.B., 1984. Early region 1B of adenovirus 2 encodes two coterminal proteins of 495 and 155 amino acid residues. J. Virol. 50 (2), 387–396.

Arnold, M.R., Kremer, W., Ludemann, H.D., Kalbitzer, H.R., 2002. 1H-NMR parameters of common amino acid residues measured in aqueous solutions of the linear tetrapeptides Gly-Gly-X-Ala at pressures between 0.1 and 200 MPa. Biophys. Chem. 96 (2–3), 129–140.

Baker, A., Rohleder, K.J., Hanakahi, L.A., Ketner, G., 2007. Adenovirus E4 34k and E1b 55k oncoproteins target host DNA ligase IV for proteasomal degradation. J. Virol. 81 (13), 7034–7040.

Bedi, G.S., Bedi, S.K., 1995. Purification and characterization of rat parotid glycosylated, basic and acidic proline-rich proteins. Prep. Biochem. 25 (3), 119–132.

Beeley, J.A., Newman, F., Wilson, P.H., Shimmin, I.C., 1996. Sodium dodecyl sulphate-polyacrylamide gel electrophoresis of human parotid salivary proteins: comparison of dansylation, coomassie blue R-250 and silver detection methods. Electrophoresis 17 (3), 505–506.

Bertani, G., 1951. Studies on lysogenesis. I. The mode of phage liberation by lysogenic *Escherichia coli*. J. Bacteriol. 62 (3), 293–300.

Bertani, G., 2004. Lysogeny at mid-twentieth century: P1, P2, and other experimental systems. J. Bacteriol. 186 (3), 595–600.

Blackford, A.N., Grand, R.J., 2009. Adenovirus E1B 55-kilodalton protein: multiple roles in viral infection and cell transformation. J. Virol. 83 (9), 4000–4012.

Blanchette, P., Cheng, C.Y., Yan, Q., Ketner, G., Ornelles, D.A., Dobner, T., Conaway, R.C., Conaway, J.W., Branton, P.E., 2004. Both BC-box motifs of adenovirus protein E4orf6 are required to efficiently assemble an E3 ligase complex that degrades p53. Mol. Cell. Biol. 24 (21), 9619–9629.

Boulant, S., Vanbelle, C., Ebel, C., Penin, F., Lavergne, J.P., 2005. Hepatitis C virus core protein is a dimeric alpha-helical protein exhibiting membrane protein features. J. Virol. 79 (17), 11353–11365.

Bradford, M.M., 1976. A rapid and sensitive method for the quantitation of microgram quantities of protein utilizing the principle of protein-dye binding. Anal. Biochem. 72, 248–254.

Brown, C.J., Takayama, S., Campen, A.M., Vise, P., Marshall, T.W., Oldfield, C.J., Williams, C.J., Dunker, A.K., 2002. Evolutionary rate heterogeneity in proteins with long disordered regions. J. Mol. Evol. 55 (1), 104–110.
Budisa, N., Steipe, B., Demange, P., Eckerskorn, C., Kellermann, J., Huber, R., 1995. High-level biosynthetic substitution of methionine in proteins by its analogs 2-aminohexanoic acid, selenomethionine, telluromethionine and ethionine in *Escherichia coli*. Eur. J. Biochem. 230 (2), 788–796.
Cheng, J., Randall, A.Z., Sweredoski, M.J., Baldi, P., 2005. SCRATCH: a protein structure and structural feature prediction server. Nucleic Acids Res. 33 (Web Server issue), W72–W76.
Chevallet, M., Luche, S., Rabilloud, T., 2006. Silver staining of proteins in polyacrylamide gels. Nat. Protoc. 1 (4), 1852–1858.
Chow, L.T., Broker, T.R., Lewis, J.B., 1979. Complex splicing patterns of RNAs from the early regions of adenovirus-2. J. Mol. Biol. 134 (2), 265–303.
Cooper, J.B., Khan, G., Taylor, G., Tickle, I.J., Blundell, T.L., 1990. X-ray analyses of aspartic proteinases. II. Three-dimensional structure of the hexagonal crystal form of porcine pepsin at 2.3 A resolution. J. Mol. Biol. 214 (1), 199–222.
Cuconati, A., White, E., 2002. Viral homologs of BCL-2: role of apoptosis in the regulation of virus infection. Genes Dev. 16 (19), 2465–2478.
Dekker, J., Kanellopoulos, P.N., van Oosterhout, J.A., Stier, G., Tucker, P.A., van der Vliet, P.C., 1998. ATP-independent DNA unwinding by the adenovirus single-stranded DNA binding protein requires a flexible DNA binding loop. J. Mol. Biol. 277 (4), 825–838.
Dosztanyi, Z., Csizmok, V., Tompa, P., Simon, I., 2005a. IUPred: web server for the prediction of intrinsically unstructured regions of proteins based on estimated energy content. Bioinformatics 21 (16), 3433–3434.
Dosztanyi, Z., Csizmok, V., Tompa, P., Simon, I., 2005b. The pairwise energy content estimated from amino acid composition discriminates between folded and intrinsically unstructured proteins. J. Mol. Biol. 347 (4), 827–839.
Dosztanyi, Z., Meszaros, B., Simon, I., 2009. ANCHOR: web server for predicting protein binding regions in disordered proteins. Bioinformatics 25 (20), 2745–2746.
Duhamel, R.C., Brendel, K., 1983. Coomassie Blue R-250 metachromatic staining of histone 5 from goose and chicken erythrocytes. Comp. Biochem. Physiol. B 75 (1), 133–135.
Duhamel, R.C., Meezan, E., Brendel, K., 1980. Metachromatic staining with Coomassie Brilliant Blue R-250 of the proline-rich calf thymus histone, H1. Biochim. Biophys. Acta 626 (2), 432–442.
Duhamel, R.C., Meezan, E., Brendel, K., 1981. The addition of SDS to the Bradford dye-binding protein assay, a modification with increased sensitivity to collagen. J. Biochem. Biophys. Methods 5 (2), 67–74.
Dunker, A.K., Lawson, J.D., Brown, C.J., Williams, R.M., Romero, P., Oh, J.S., Oldfield, C.J., Campen, A.M., Ratliff, C.M., Hipps, K.W., Ausio, J., Nissen, M.S., Reeves, R., Kang, C., Kissinger, C.R., Bailey, R.W., Griswold, M.D., Chiu, W., Garner, E.C., Obradovic, Z., 2001. Intrinsically disordered protein. J. Mol. Graph. Model. 19 (1), 26–59.
Dunker, A.K., Brown, C.J., Lawson, J.D., Iakoucheva, L.M., Obradovic, Z., 2002. Intrinsic disorder and protein function. Biochemistry 41 (21), 6573–6582.
Dunker, A.K., Cortese, M.S., Romero, P., Iakoucheva, L.M., Uversky, V.N., 2005. Flexible nets. The roles of intrinsic disorder in protein interaction networks. FEBS J. 272 (20), 5129–5148.
Dyson, H.J., Wright, P.E., 2002. Insights into the structure and dynamics of unfolded proteins from nuclear magnetic resonance. Adv. Protein Chem. 62, 311–340.
Farrow, N.A., Muhandiram, R., Singer, A.U., Pascal, S.M., Kay, C.M., Gish, G., Shoelson, S.E., Pawson, T., Forman-Kay, J.D., Kay, L.E., 1994. Backbone dynamics of a free and phosphopeptide-complexed Src homology 2 domain studied by 15N NMR relaxation. Biochemistry 33 (19), 5984–6003.
Ferreon, J.C., Martinez-Yamout, M.A., Dyson, H.J., Wright, P.E., 2009. Structural basis for subversion of cellular control mechanisms by the adenoviral E1A oncoprotein. Proc. Natl. Acad. Sci. U. S. A. 106 (32), 13260–13265.
Fleisig, H.B., Orazio, N.I., Liang, H., Tyler, A.F., Adams, H.P., Weitzman, M.D., Nagarajan, L., 2007. Adenoviral E1B55K oncoprotein sequesters candidate leukemia suppressor sequence-specific single-stranded DNA-binding protein 2 into aggresomes. Oncogene 26 (33), 4797–4805.
Friedman, R.D., 1982. Comparison of four different silver-staining techniques for salivary protein detection in alkaline polyacrylamide gels. Anal. Biochem. 126 (2), 346–349.
Galea, C.A., Wang, Y., Sivakolundu, S.G., Kriwacki, R.W., 2008. Regulation of cell division by intrinsically unstructured proteins: intrinsic flexibility, modularity, and signaling conduits. Biochemistry 47 (29), 7598–7609.
Gersten, D.M., Rodriguez, L.V., George, D.G., Johnston, D.A., Zapolski, E.J., 1991. On the relationship of amino acid composition to silver staining of proteins in electrophoresis gels: II. Peptide sequence analysis. Electrophoresis 12 (6), 409–414.
Gey, G.O., Coffman, W.D., Kubicek, M.T., 1952. Tissue culture studies of the proliferative capacity of cervical carcinoma and normal epithelium. Cancer Res. 12, 264–265.
Gill, S.C., von Hippel, P.H., 1989. Calculation of protein extinction coefficients from amino acid sequence data. Anal. Biochem. 182 (2), 319–326.
Graziano, V., Gerchman, S.E., Wonacott, A.J., Sweet, R.M., Wells, J.R., White, S.W., Ramakrishnan, V., 1990. Crystallization of the globular domain of histone H5. J. Mol. Biol. 212 (2), 253–257.
Green, M., Brackmann, K.H., Cartas, M.A., Matsuo, T., 1982. Identification and purification of a protein encoded by the human adenovirus type 2 transforming region. J. Virol. 42 (1), 30–41.
Gronwald, W., Kalbitzer, H.R., 2004. Automated structure determination of proteins by NMR spectroscopy. Prog. NMR Spectr. 44 (1–2), 33–96.
Gronwald, W., Huber, F., Grunewald, P., Sporner, M., Wohlgemuth, S., Herrmann, C., Kalbitzer, H.R., 2001. Solution structure of the Ras binding domain of the protein kinase Byr2 from *Schizosaccharomyces pombe*. Structure 9 (11), 1029–1041.
Habchi, J., Mamelli, L., Darbon, H., Longhi, S., 2010. Structural disorder within Henipavirus nucleoprotein and phosphoprotein: from predictions to experimental assessment. PLoS One 5 (7), e11684.
Harada, J.N., Shevchenko, A., Shevchenko, A., Pallas, D.C., Berk, A.J., 2002. Analysis of the adenovirus E1B-55K-anchored proteome reveals its link to ubiquitination machinery. J. Virol. 76 (18), 9194–9206.
Hattori, S., Sakai, K., Watanabe, K., Fujii, T., 1996. The induction of metachromasia and circular dichroism of coomassie brilliant blue R-250 with collagen and histone H1 is due to the low content of hydrophobic amino acid residues in these proteins. J. Biochem. 119 (3), 400–406.
Hayashi, T., Nagai, Y., 1980. The anomalous behavior of collagen peptides on sodium dodecyl sulfate-polyacrylamide gel electrophoresis is due to the low content of hydrophobic amino acid residues. J. Biochem. 87 (3), 803–808.
Johnson Jr., W.C., 1990. Protein secondary structure and circular dichroism: a practical guide. Proteins 7 (3), 205–214.
Jones, D.T., 1999. Protein secondary structure prediction based on position-specific scoring matrices. J. Mol. Biol. 292 (2), 195–202.
Jones, N., Shenk, T., 1979. Isolation of adenovirus type 5 host range deletion mutants defective for transformation of rat embryo cells. Cell 17 (3), 683–689.
Karlin, D., Longhi, S., Receveur, V., Canard, B., 2002. The N-terminal domain of the phosphoprotein of Morbilliviruses belongs to the natively unfolded class of proteins. Virology 296 (2), 251–262.
Kindsmuller, K., Schreiner, S., Leinenkugel, F., Groitl, P., Kremmer, E., Dobner, T., 2009. A 49-kilodalton isoform of the adenovirus type 5 early region 1B 55-kilodalton protein is sufficient to support virus replication. J. Virol. 83 (18), 9045–9056.
Kovacs, E., Tompa, P., Liliom, K., Kalmar, L., 2010. Dual coding in alternative reading frames correlates with intrinsic protein disorder. Proc. Natl. Acad. Sci. U. S. A. 107 (12), 5429–5434.
Leppard, K.N., Everett, R.D., 1999. The adenovirus type 5 E1b 55K and E4 Orf3 proteins associate in infected cells and affect ND10 components. J. Gen. Virol. 80 (Pt 4), 997–1008.
Lewis, J.B., Anderson, C.W., 1987. Identification of adenovirus type 2 early region 1B proteins that share the same amino terminus as do the 495R and 155R proteins. J. Virol. 61 (12), 3879–3888.
Linding, R., Jensen, L.J., Diella, F., Bork, P., Gibson, T.J., Russell, R.B., 2003. Protein disorder prediction: implications for structural proteomics. Structure 11 (11), 1453–1459.
Longhi, S., Receveur-Brechot, V., Karlin, D., Johansson, K., Darbon, H., Bhella, D., Yeo, R., Finet, S., Canard, B., 2003. The C-terminal domain of the measles virus nucleoprotein is intrinsically disordered and folds upon binding to the C-terminal moiety of the phosphoprotein. J. Biol. Chem. 278 (20), 18638–18648.
Loomis, R.E., Bergey, E.J., Levine, M.J., Tabak, L.A., 1985. Circular dichroism and fluorescence spectroscopic analyses of a proline-rich glycoprotein from human parotid saliva. Int. J. Pept. Protein Res. 26 (6), 621–629.
Lucher, L.A., Brackmann, K.H., Symington, J.S., Green, M., 1984. Antibody directed to a synthetic peptide encoding the NH2-terminal 16 amino acids of the adenovirus type 2 E1B-53K tumor antigen recognizes the E1B-20K tumor antigen. Virology 132 (1), 217–221.
Maheswaran, S., Englert, C., Lee, S.B., Ezzel, R.M., Settleman, J., Haber, D.A., 1998. E1B 55K sequesters WT1 along with p53 within a cytoplasmic body in adenovirus-transformed kidney cells. Oncogene 16 (16), 2041–2050.
Marshall, T., 1984. Analysis of human sweat proteins by two-dimensional electrophoresis and ultrasensitive silver staining. Anal. Biochem. 139 (2), 506–509.
Marton, M.J., Baim, S.B., Ornelles, D.A., Shenk, T., 1990. The adenovirus E4 17-kilodalton protein complexes with the cellular transcription factor E2F, altering its DNA-binding properties and stimulating E1A-independent accumulation of E2 mRNA. J. Virol. 64 (5), 2345–2359.
Mayor, U., Guydosh, N.R., Johnson, C.M., Grossmann, J.G., Sato, S., Jas, G.S., Freund, S.M., Alonso, D.O., Daggett, V., Fersht, A.R., 2003. The complete folding pathway of a protein from nanoseconds to microseconds. Nature 421 (6925), 863–867.
McCormick, P.J., Chandrasekhar, S., Millis, A.J., 1979. Direct visualization of collagens and procollagens in polyacrylamide gels. Anal. Biochem. 97 (2), 359–366.
Micko, S., Schlaepfer, W.W., 1978. Metachromasy of peripheral nerve collagen on polyacrylamide gels stained with Coomassie brilliant blue R-250. Anal. Biochem. 88 (2), 566–572.
Mohammadi, E.S., Ketner, E.A., Johns, D.C., Ketner, G., 2004. Expression of the adenovirus E4 34k oncoprotein inhibits repair of double strand breaks in the cellular genome of a 293-based inducible cell line. Nucleic Acids Res. 32 (8), 2652–2659.
Montell, C., Fisher, E.F., Caruthers, M.H., Berk, A.J., 1984. Control of adenovirus E1B mRNA synthesis by a shift in the activities of RNA splice sites. Mol. Cell. Biol. 4 (5), 966–972.
Morrissey, J.H., 1981. Silver stain for proteins in polyacrylamide gels: a modified procedure with enhanced uniform sensitivity. Anal. Biochem. 117 (2), 307–310.
Nielsen, B.L., Brown, L.R., 1984. The basis for colored silver–protein complex formation in stained polyacrylamide gels. Anal. Biochem. 141 (2), 311–315.
Orazio, N.I., Naeger, C.M., Karlseder, J., Weitzman, M.D., 2011. The adenovirus E1b55K/E4orf6 complex induces degradation of the Bloom helicase during infection. J. Virol. 85 (4), 1887–1892.
Pelka, P., Ablack, J.N., Fonseca, G.J., Yousef, A.F., Mymryk, J.S., 2008. Intrinsic structural disorder in adenovirus E1A: a viral molecular hub linking multiple diverse processes. J. Virol. 82 (15), 7252–7263.
Peng, K., Vucetic, S., Radivojac, P., Brown, C.J., Dunker, A.K., Obradovic, Z., 2005. Optimizing long intrinsic disorder predictors with protein evolutionary information. J. Bioinform. Comput. Biol. 3 (1), 35–60.
Petersen, B., Petersen, T.N., Andersen, P., Nielsen, M., Lundegaard, C., 2009. A generic method for assignment of reliability scores applied to solvent accessibility predictions. BMC Struct. Biol. 9, 51.

Pirovano, W., Heringa, J., 2010. Protein secondary structure prediction. Methods Mol. Biol. 609, 327–348.
Plowman, J.E., Bryson, W.G., Jordan, T.W., 2000. Application of proteomics for determining protein markers for wool quality traits. Electrophoresis 21 (9), 1899–1906.
Querido, E., Blanchette, P., Yan, Q., Kamura, T., Morrison, M., Boivin, D., Kaelin, W.G., Conaway, R.C., Conaway, J.W., Branton, P.E., 2001. Degradation of p53 by adenovirus E4orf6 and E1B55K proteins occurs via a novel mechanism involving a Cullin-containing complex. Genes Dev. 15 (23), 3104–3117.
Rabilloud, T., 1990. Mechanisms of protein silver staining in polyacrylamide gels: a 10-year synthesis. Electrophoresis 11 (10), 785–794.
Rabilloud, T., Vuillard, L., Gilly, C., Lawrence, J.J., 1994. Silver-staining of proteins in polyacrylamide gels: a general overview. Cell. Mol. Biol. (Noisy-le-Grand) 40 (1), 57–75.
Rancurel, C., Khosravi, M., Dunker, A.K., Romero, P.R., Karlin, D., 2009. Overlapping genes produce proteins with unusual sequence properties and offer insight into de novo protein creation. J. Virol. 83 (20), 10719–10736.
Receveur-Brechot, V., Bourhis, J.M., Uversky, V.N., Canard, B., Longhi, S., 2006. Assessing protein disorder and induced folding. Proteins 62 (1), 24–45.
Romero, P., Obradovic, Z., Kissinger, C.R., Villafranca, J.E., Garner, E., Guilliot, S., Dunker, A.K., 1998. Thousands of proteins likely to have long disordered regions. Pac. Symp. Biocomput. 437–448.
Romero, P.R., Zaidi, S., Fang, Y.Y., Uversky, V.N., Radivojac, P., Oldfield, C.J., Cortese, M.S., Sickmeier, M., LeGall, T., Obradovic, Z., Dunker, A.K., 2006. Alternative splicing in concert with protein intrinsic disorder enables increased functional diversity in multicellular organisms. Proc. Natl. Acad. Sci. U. S. A. 103 (22), 8390–8395.
Roy, A., Kucukural, A., Zhang, Y., 2010. I-TASSER: a unified platform for automated protein structure and function prediction. Nat. Protoc. 5 (4), 725–738.
Rubenwolf, S., Schütt, H., Nevels, M., Wolf, H., Dobner, T., 1997. Structural analysis of the adenovirus type 5 E1B 55-kilodalton–E4orf6 protein complex. J. Virol. 71 (2), 1115–1123.
Sam, M.D., Papagiannis, C.V., Connolly, K.M., Corselli, L., Iwahara, J., Lee, J., Phillips, M., Wojciak, J.M., Johnson, R.C., Clubb, R.T., 2002. Regulation of directionality in bacteriophage lambda site-specific recombination: structure of the Xis protein. J. Mol. Biol. 324 (4), 791–805.
Sarnow, P., Sullivan, C.A., Levine, A.J., 1982. A monoclonal antibody detecting the adenovirus type 5-E1b-58Kd tumor antigen: characterization of the E1b-58Kd tumor antigen in adenovirus-infected and -transformed cells. Virology 120 (2), 510–517.
Schreiner, S., Wimmer, P., Sirma, H., Everett, R.D., Blanchette, P., Groitl, P., Dobner, T., 2010. Proteasome-dependent degradation of Daxx by the viral E1B-55K protein in human adenovirus-infected cells. J. Virol. 84 (14), 7029–7038.
Shatzman, A.R., Henkin, R.I., 1983. The proline-, glycine-, glutamic acid-rich pink-violet staining proteins in human parotid saliva are phosphoproteins. Biochem. Med. 29 (2), 182–193.
Shenk, T., 2001. *Adenoviridae:* The viruses and their replication. 4 Raven Press, New York, N.Y.
Sieber, T., Dobner, T., 2007. Adenovirus type 5 early region 1B 156R protein promotes cell transformation independently of repression of p53-stimulated transcription. J. Virol. 81 (1), 95–105.
Spector, D.J., McGrogan, M., Raskas, H.J., 1978. Regulation of the appearance of cytoplasmic RNAs from region 1 of the adenovirus 2 genome. J. Mol. Biol. 126 (3), 395–414.
Stracker, T.H., Carson, C.T., Weitzman, M.D., 2002. Adenovirus oncoproteins inactivate the Mre11-Rad50-NBS1 DNA repair complex. Nature 418 (6895), 348–352.
Stump, M.R., Gloss, L.M., 2008. Mutational analysis of the stability of the H2A and H2B histone monomers. J. Mol. Biol. 384 (5), 1369–1383.
Szollosi, E., Hazy, E., Szasz, C., Tompa, P., 2007. Large systematic errors compromise quantitation of intrinsically unstructured proteins. Anal. Biochem. 360 (2), 321–323.
Takayesu, D., Teodoro, J.G., Whalen, S.G., Branton, P.E., 1994. Characterization of the 55K adenovirus type 5 E1B product and related proteins. J. Gen. Virol. 75 (Pt 4), 789–798.
Tal, M., Silberstein, A., Nusser, E., 1985. Why does Coomassie Brilliant Blue R interact differently with different proteins? A partial answer. J. Biol. Chem. 260 (18), 9976–9980.
Tamiola, K., Acar, B., Mulder, F.A., 2010. Sequence-specific random coil chemical shifts of intrinsically disordered proteins. J. Am. Chem. Soc. 132 (51), 18000–18003.
Tompa, P., 2002. Intrinsically unstructured proteins. Trends Biochem. Sci. 27 (10), 527–533.
Tucker, P.A., Tsernoglou, D., Tucker, A.D., Coenjaerts, F.E., Leenders, H., van der Vliet, P.C., 1994. Crystal structure of the adenovirus DNA binding protein reveals a hook-on model for cooperative DNA binding. EMBO J. 13 (13), 2994–3002.
Uversky, V.N., 2002. Natively unfolded proteins: a point where biology waits for physics. Protein Sci. 11 (4), 739–756.
Uversky, V.N., 2009. Intrinsically disordered proteins and their environment: effects of strong denaturants, temperature, pH, counter ions, membranes, binding partners, osmolytes, and macromolecular crowding. Protein J. 28 (7–8), 305–325.
Uversky, V.N., Gillespie, J.R., Fink, A.L., 2000. Why are "natively unfolded" proteins unstructured under physiologic conditions? Proteins 41 (3), 415–427.
van Breukelen, B., Kanellopoulos, P.N., Tucker, P.A., van der Vliet, P.C., 2000. The formation of a flexible DNA-binding protein chain is required for efficient DNA unwinding and adenovirus DNA chain elongation. J. Biol. Chem. 275 (52), 40897–40903.
Vila, R., Ponte, I., Jimenez, M.A., Rico, M., Suau, P., 2000. A helix-turn motif in the C-terminal domain of histone H1. Protein Sci. 9 (4), 627–636.
Vila, R., Ponte, I., Collado, M., Arrondo, J.L., Suau, P., 2001. Induction of secondary structure in a COOH-terminal peptide of histone H1 by interaction with the DNA: an infrared spectroscopy study. J. Biol. Chem. 276 (33), 30898–30903.
Virtanen, A., Pettersson, U., 1985. Organization of early region 1B of human adenovirus type 2: identification of four differentially spliced mRNAs. J. Virol. 54 (2), 383–391.
Vucetic, S., Brown, C.J., Dunker, A.K., Obradovic, Z., 2003. Flavors of protein disorder. Proteins 52 (4), 573–584.
Wang, Y., Jardetzky, O., 2002. Probability-based protein secondary structure identification using combined NMR chemical-shift data. Protein Sci. 11 (4), 852–861.
White, E., 2001. Regulation of the cell cycle and apoptosis by the oncogenes of adenovirus. Oncogene 20 (54), 7836–7846.
Wilson, M.C., Darnell Jr., J.E., 1981. Control of messenger RNA concentration by differential cytoplasmic half-life. Adenovirus messenger RNAs from transcription units 1A and 1B. J. Mol. Biol. 148 (3), 231–251.
Wimmer, P., Schreiner, S., Everett, R.D., Sirma, H., Groitl, P., Dobner, T., 2010. SUMO modification of E1B-55K oncoprotein regulates isoform-specific binding to the tumour suppressor protein PML. Oncogene 29 (40), 5511–5522.
Wishart, D.S., Sykes, B.D., Richards, F.M., 1991. Simple techniques for the quantification of protein secondary structure by 1H NMR spectroscopy. FEBS Lett. 293 (1–2), 72–80.
Wishart, D.S., Bigam, C.G., Yao, J., Abildgaard, F., Dyson, H.J., Oldfield, E., Markley, J.L., Sykes, B.D., 1995. 1H, 13C and 15N chemical shift referencing in biomolecular NMR. J. Biomol. NMR 6 (2), 135–140.
Wojciak, J.M., Sarkar, D., Landy, A., Clubb, R.T., 2002. Arm-site binding by lambda -integrase: solution structure and functional characterization of its amino-terminal domain. Proc. Natl. Acad. Sci. U. S. A. 99 (6), 3434–3439.
Xue, B., Williams, R.W., Oldfield, C.J., Goh, G.K., Dunker, A.K., Uversky, V.N., 2010. Viral disorder or disordered viruses: do viral proteins possess unique features? Protein Pept. Lett. 17 (8), 932–951.
Yang, Z.R., Thomson, R., McNeil, P., Esnouf, R.M., 2005. RONN: the bio-basis function neural network technique applied to the detection of natively disordered regions in proteins. Bioinformatics 21 (16), 3369–3376.
Ye, Y., Godzik, A., 2003. Flexible structure alignment by chaining aligned fragment pairs allowing twists. Bioinformatics 19 (Suppl 2), ii246–ii255.
Yew, P.R., Berk, A.J., 1992. Inhibition of p53 transactivation required for transformation by adenovirus early 1B protein. Nature 357 (6373), 82–85.
Yüksel, K.Ü., Gracy, R.W., 1985. The quantitation of proteins in silver stained polyacrylamide gels. Electrophoresis 6, 361–366.
Zhang, Y., 2007. Template-based modeling and free modeling by I-TASSER in CASP7. Proteins 69 (Suppl 8), 108–117.
Zhang, Y., 2008. I-TASSER server for protein 3D structure prediction. BMC Bioinformatics 9, 40.
Zhou, R., Wolk, C.P., 2002. Identification of an akinete marker gene in *Anabaena variabilis*. J. Bacteriol. 184 (9), 2529–2532.